

Cite this article as:

Kang B, Kim M, Song S, Jun Dwon, Jang K. Feasibility of modified Dixon MRI techniques for hepatic fat quantification in hepatic disorders: validation with MRS and histology. *Br J Radiol* 2018; **90**: 20170378.

THE ROLE OF IMAGING IN OBESITY SPECIAL FEATURE: FULL PAPER

Feasibility of modified Dixon MRI techniques for hepatic fat quantification in hepatic disorders: validation with MRS and histology

¹BO-KYEONG KANG, ¹MIMI KIM, ¹SOON-YOUNG SONG, ²DAE WON JUN and ³KISEOK JANG

¹Department of Radiology, Hanyang University School of Medicine, Hanyang University Medical Center, Seoul, Korea

²Department of Internal Medicine, Hanyang University School of Medicine, Hanyang University Medical Center, Seoul, Korea

³Department of Pathology, Hanyang University School of Medicine, Hanyang University Medical Center, Seoul, Korea,

Address correspondence to: Dr Dae won Jun

E-mail: noshin@hanyang.ac.kr

The authors Bo-Kyeong Kang and Mimi Kim contributed equally to the work.

Objective: To assess the feasibility of proton density fat fraction (PDFFF) MRI for estimating hepatic fat fraction with magnetic resonance spectroscopy (MRS) and histology as references and to investigate intrahepatic fat distribution and variability.

Methods: Between November 2014 and September 2015, 85 adults (48 males, 47 females) who underwent MRI-PDFF ($n = 139$), MRS-PDFF ($n = 49$) and liver biopsy ($n = 29$) were enrolled in this study. Data were compared using linear regression. MRI-PDFF and standard deviations (variability) and differences between maximum and minimum PDFFF (PDFFF range) for whole liver, the lobes, and segment levels were calculated for each subject.

Results: Whole-liver MRI-PDFF showed good correlation with MRS-PDFF ($r = 0.961$) and histologic degree

of hepatic steatosis ($\sigma = 0.809$). Hepatic fat fraction is different between lobes and segments. Mean PDFFF and mean PDFFF range of the right lobe were higher than for the left lobe, whereas variability in the right lobe was lower than in the left lobe.

Conclusion: MRI-PDFF is an accurate non-invasive method for quantifying hepatic fat for various hepatic disorders, and may be preferable for measuring fat fraction in the right liver for more precise values in longitudinal monitoring, while avoiding FF measurement in the left liver.

Advances in knowledge: MRI-PDFF provides a non-invasive and accurate quantification of hepatic steatosis in various hepatic disorders. It would be preferable to measure FF in the right liver than in the left liver.

INTRODUCTION

Non-alcoholic fatty liver disease (NAFLD) is a common type of liver disease, globally affecting 25.2% with highest prevalence in the Middle East and South America.¹ In alcoholic and NAFLD, hepatic steatosis can progress to steatohepatitis, advanced fibrosis, and cirrhosis, and can increase hepatocellular carcinoma risk. NAFLD is also a major risk factor for cardiovascular disease² and can influence the outcome of liver transplantation, not only for the recipient, but also for the living donor after partial hepatectomy.^{3,4} Therefore, accurate assessment of steatosis may be important in determining appropriate therapeutic interventions to prevent long-term complications.

Liver biopsy has been the reference standard for diagnosing and grading of steatosis; however, it is invasive, can cause sampling biases, and is vulnerable to high interobserver variability.^{5,6} Therefore, alternative non-invasive methods would be beneficial.

In recent years, significant advances have been made in accurate quantification of liver fat.⁷ Among the non-invasive quantification methods, magnetic resonance spectroscopy (MRS) has been accepted as the most accurate non-invasive technique, but it is restricted in its spatial coverage and is difficult to perform and analyse. MRI measuring proton density fat fraction (PDFFF) is a promising method for covering the entire liver volume in a single breath hold, making it a practical alternative to MRS. Furthermore,

each major vendor provides a specific sequence for fat quantification, such as IDEAL IQ (GE Healthcare, Milwaukee, WI), mDIXON-Quant (Philips Healthcare, Best, Netherlands) and Multiecho Dixon VIBE of LiverLab (Siemens Medical Solutions, Erlangen, Germany). These technical advantages make it easy to measure numerous areas and to cover the entire liver. However, these new sequences have not been fully validated in populations worldwide.

Steatosis tends to be diffuse, but the distribution of fat accumulation can be non-uniform across the liver.^{8,9} Several studies reported hepatic fat distribution using MRI-PDFF with various sampling methods.^{10–12} However, it has not been fully described for various hepatic disorders. More detailed descriptions of hepatic fat distribution may help inform future clinical trial designs.

The main aim of this study was to assess the feasibility of MRI (mDIXON-Quant) for estimating hepatic fat quantification using MRI with MRS and histology as references and to investigate the intrahepatic fat distribution and variability in patients with various hepatic disorders.

METHODS AND MATERIALS

Study population

This prospective single-centre clinical study was approved by University Hospital's institutional review board, and written informed consent was obtained from each patient prior to participation. The study population included subjects with one of various hepatic disorders or who were referred to our hospital for evaluation for suspected liver disease.

Between November 2014 and September 2015, 85 subjects were enrolled in this study. All 85 subjects underwent PDFF (mDIXON-Quant) with or without MRS. Among them, 29 subjects with suspected liver disease underwent PDFF and percutaneous ultrasonography-guided liver biopsy on the same day. After 3 months, 54 of 85 subjects underwent follow-up MRI, resulting in 139 MRI examinations and 54 MRS examinations for 85 subjects. Five of the 54 MRS examinations were excluded because of technical errors and failure to complete MRS. Finally, we obtained 139 MRI examinations and 49 MRS examinations.

MRI examination

All MRI and MRS examinations were performed on a 3T MRI scanner (Ingenia; Philips Healthcare, Best, Netherlands) using a 32-channel torso phased-array coil.

MRI

An axial three-dimensional multiecho modified Dixon gradient echo sequence (mDIXON-Quant) was used for steatosis evaluation. Imaging parameters for the mDIXON-Quant sequence were: six TEs [first TE shortest automatic (0.9–1.2 ms), delta TE 0.8–1.01 ms]; TR shortest automatic (5.8–6.3 ms); flip angle = 3; field of view = 35 × 35 cm; 3 mm slice thickness with no gap; matrix size = 300 × 300; Field of view 350 × 350 mm; number of slices = 60; scan time = 14.1 s; default parallel imaging SENSE factor of 2 in the anterior posterior direction, a factor of 1 in the

slice encoding direction; number of signal average = 1. mDIXON-Quant sequence automatically produces water, fat, fat fraction, R2*, and T2* maps.

MRS

Using three-plane localizing images, a single 15 × 15 × 15 mm voxel was localized in the right lobe of the liver, avoiding all liver boundaries and large vessels. After shimming, single-voxel MRS was performed using a stimulated-echo acquisition mode. During a 15-s single breath hold, 5 spectra were collected at TEs of 20, 30, 40, 50 and 60 ms. To minimize the T₁ effect, TR was set at 3000 ms. Other parameters were 10-ms mixing time, 2048 data points over a 1000 Hz receiver bandwidth.

Image analysis

MR imaging

To estimate hepatic PDFF, the signal intensities from regions of interest (ROIs) in the liver were calculated in a fat-fraction map image. Using the Philips Interspace Portal (Philips Healthcare, Best, Netherlands), all subjects' fat-fraction map images were reviewed by a single reader (with 5-year experience analysing abdomen MRI) who was blinded to all clinical, demographic and histopathologic information. Non-overlapping circular ROIs that were 100 mm² in area were taken from each Couinaud liver segment and care was taken to ensure they were devoid of large vessels, ducts, organ boundaries, focal hepatic lesions and imaging artefacts. A total of 24 ROIs per subject were obtained, including 12 from the right lobe (segments V, VI, VII and VIII) and 12 from the left lobe (segments I, II, III and IV). The average from three measurements was used as the representative hepatic PDFF for each hepatic segment.

MRS

Using Philips software (Philips Healthcare), MRS data were interpreted by a single reader (with 5-year experience analysing MRS) who was blinded to MRI and histologic results. For fat measurements, localized proton nuclear magnetic resonance spectra of the liver were acquired using a previously described method.¹³ MRS-PDFF was calculated as the area of peak fat divided by the sum of the peak water and fat areas, multiplied by 100.

Liver biopsy and histopathologic examination

Ultrasonography-guided liver biopsies were performed on 29 subjects using an 18-gauge needle (Stericut 18G coaxial; TSK Laboratory, Tochigi, Japan). Two parenchyma cores were obtained from two sites in the right anterior segment of the liver in each patient. The liver biopsy specimen was routinely processed and stained with haematoxylin–eosin. A single experienced pathologist who was blinded to the hepatic fat fraction results reviewed the biopsy. The degree of steatosis was visually assessed by estimating the percentage of hepatocytes that contained macrovesicular fat droplets. The grading system for liver steatosis was based on the NASH-CRN scoring system: Grade 1: <5% steatosis; Grade 1: 5–33% steatosis; Grade 2: 34–66% steatosis; Grade 3: >66% steatosis.¹³

Statistical analysis

Correlation between the histologic degree of steatosis vs MRI-PDFFs and MRS vs MRI-PDFFs were estimated using

Table 1. Patient characteristics ($n = 85$)

Patient characteristics	Value
Age, years ^a	47.3 ± 14.9 (15–78)
Sex	
Male	48 (56.5)
Female	37 (43.5)
Various hepatic disorders	
Non-alcoholic fatty liver disease	40 (47.0)
Alcoholic liver disease	14 (16.5)
Liver cirrhosis ^b	10 (11.8)
Toxic hepatitis	7 (8.2)
Malignant disease ^c	6 (7.1)
No definite diagnostic change in the liver on biopsy ^d	4 (4.6)
Autoimmune hepatitis	2 (2.4)
Acute viral hepatitis	1 (1.2)
Chronic viral hepatitis	1 (1.2)

Note: Data are presented as number of patients with percentages in parentheses, unless indicated otherwise.

^aData are presented as mean ±SD with ranges in parentheses.

^bLiver cirrhosis, including alcoholic liver disease ($n = 6$), chronic viral hepatitis ($n = 4$).

^cMalignant disease, including hepatocellular carcinoma ($n = 1$), diffuse large B cell lymphoma ($n = 1$), metastatic adenocarcinoma ($n = 3$), melanoma ($n = 1$).

^dNo definite diagnostic change in the liver, including minimal portal or lobular inflammation.

Spearman correlation test, Pearson's correlation analysis with Bland-Altman analysis. The mean and variability (SD) of PDFF for the whole liver, the lobar and segment levels were calculated for each subject. The mean differences between the maximum and minimum hepatic PDFF (PDFF range) for the whole liver, the lobar, and segment levels were also calculated. The relationships between hepatic PDFF and PDFF range were assessed using Pearson's correlation coefficient for the univariate analyses. Mixed model and repeated-measures of analyses of variance were used to assess differences in mean and variability between segments. All statistical analyses were conducted using commercial software (IBM SPSS v. 21, IBM, Armonk, NY; MedCalc v. 17.2 (MedCalc Software, Ostend, Belgium); SAS version 9.4 (SAS Institute Inc., Cary, NC). A p -value < 0.05 was considered statistically significant.

RESULTS

Characteristics of the study population

The study population consisted of 48 males and 37 females (mean age: 47.3 years ± 14.9; range: 15–78 years). 56 of the study patients (NAFLD, $n = 34$; alcoholic liver disease, $n = 13$; liver cirrhosis, $n = 9$) treated for over 2 years were included. 29 patients with suspected liver disease underwent ultrasonography-guided percutaneous liver biopsy were also included. Detailed pathologies are described in Table 1.

Correlation between MRI-PDFF and histologic degree of steatosis

Right-lobe PDFF was more strongly correlated with histologic degree of steatosis than left-lobe PDFF ($\sigma = 0.811$, $p < 0.001$ for the right lobe, $\sigma = 0.805$, $p < 0.001$ for the left lobe). Whole-liver PDFF also showed excellent correlation with histology degree ($\sigma = 0.809$, $p < 0.001$). The relationships between MRI-PDFF and histologic degree of steatosis are presented in Figure 1.

Correlation between MRI and MRS

The relationships between PDFF measured by MRI and MRS are presented in Table 2 and Figure 2. In Pearson's correlation analysis, MRI-PDFF showed a higher correlation with MRS-PDFF in the right lobe than in the left lobe ($r = 0.970$, $p < 0.001$ for the right lobe, $r = 0.944$, $p < 0.001$ for the left lobe). Segment VI PDFF showed the strongest correlation with MRS-PDFF ($r = 0.972$, $p < 0.001$), followed by segment V PDFF ($r = 0.969$, $p < 0.001$) and segment VII PDFF ($r = 0.966$, $p < 0.001$). Bland-Altman analysis displayed fat fraction of MRI of whole liver, right liver, left liver and segment VI tend to be underestimated compared with MRS as mean of fat fraction increased.

Intrahepatic fat distribution and variability measured by MRI

Intrahepatic fat distribution and variability measured by MRI for the whole liver, the lobar and segmental levels are summarized in Table 3. Mean whole-liver PDFF was 14.3% (range: 1.1–46.7%) while mean whole-liver PDFF variability was 1.68% (range: 0.54–6.39%). Whole-liver PDFF variability and whole-liver PDFF range increased as whole-liver PDFF increased ($r = 0.588$; $p < 0.001$ for whole-liver PDFF variability, $r = 0.499$; $p < 0.001$ for whole-liver PDFF range).

Right-lobe PDFF was higher than left-lobe PDFF (14.9% for the right lobe vs 13.8% for the left lobe, $p < 0.001$), whereas right-lobe variability was lower than left-lobe PDFF variability (1.15% for the right lobe vs 1.74% for the left lobe, $p < 0.001$). Right-lobe PDFF range was also lower than left-lobe PDFF range (2.4% for the right lobe vs 3.5% for the left lobe).

Segment VI had the highest mean segmental PDFF (15.1%, range: 1–46.4%), whereas segment II had the lowest mean segmental PDFF (13%, range 0.2–48.3%) ($p < 0.001$). And segment VI had the lowest segmental PDFF variability (0.66%, range 0–2.54%), whereas segment III had the highest mean segmental PDFF variability (1.19%, range 0.06–6.23%) ($p < 0.001$) (Supplementary Table 1). Segment PDFF range was highest in segment III (2.3%, range 0.1–28.7%) and lowest in segment VI (1.3%, range 0.1–4.3%).

DISCUSSION

Our study evaluated a modified Dixon technique (mDIXON-Quant) for hepatic fat quantification in patients with various hepatic disorders. We compared this technique to MRS and histology. Our results demonstrated that MRI-PDFF using mDIXON-Quant showed excellent correlation with MRS-PDFF

Table 2. Correlation between MRI and MRS ($n = 49$)

		MRS	
		R	p^a
MRI	Whole liver	0.961	<0.001
	Lobe		
	Right	0.970	<0.001
	Left	0.944	<0.001
	Segment		
	I	0.927	<0.001
	II	0.935	<0.001
	III	0.924	<0.001
IV	0.943	<0.001	
V	0.969	<0.001	
VI	0.972	<0.001	
VII	0.966	<0.001	
VIII	0.956	<0.001	

MRS, magnetic resonance spectroscopy.

^a $p < 0.05$ by Pearson correlation.

and histology in Pearson correlation analysis and Spearman correlation test, respectively. Our findings are consistent with those of previous studies.^{12,14-16} However, MRI is underestimating fat fraction compared to MRS as mean of fat fraction increased in Bland-Altman analysis. Martino et al showed a similar result with our study.¹⁷ A possible explanation is limitation of chemical shift technique which is unreliable for discrimination of moderate and severe fatty liver. Nevertheless, MRI is useful for longitudinal monitoring in clinical settings because of high value of correlation coefficient of fat fraction with MRS, convenience to perform without invasiveness and full coverage of whole liver.

Although MRS has been generally accepted as the most accurate non-invasive method for hepatic fat quantification, it has several limitations regarding its clinical application: it requires a skilled technologist to collect the data and specific analysis software to analyse those data; sampling errors are common due to small sampling volumes; it cannot cover the whole liver; it involves a long acquisition time; and it has high cost. Therefore, to measure hepatic PDFF, MRI became the focus of attention as an alternative method of MRS. Several studies found that MRI-PDFF yielded high overall accuracy compared with MRS and histology.^{11,14,18-20} Our study used a commercially available sequence from a major MRI manufacturer for hepatic fat quantification. It is expected to become widely available as a clinical and research tool for detection and monitoring of steatosis. The correlation coefficient of right liver is higher than left liver. It may be related to measuring of MRS was undertaken in a single liver voxel of right liver. But, other value is also high as 0.9 or higher.

Histologic evaluation of diffuse liver disease still has a significant diagnostic role when evaluating other features, such as

Figure 1. Scatterplots showing mean fat fraction measured by MRI and histologic degree of hepatic steatosis: (a) whole-liver PDFF, (b) right-lobe PDFF and (c) left-lobe PDFF showed excellent agreement with histologic degree of hepatic steatosis ($\sigma = 0.920$, $\sigma = 0.930$ and $\sigma = 0.905$, respectively). PDFF, protondensity fat fraction.

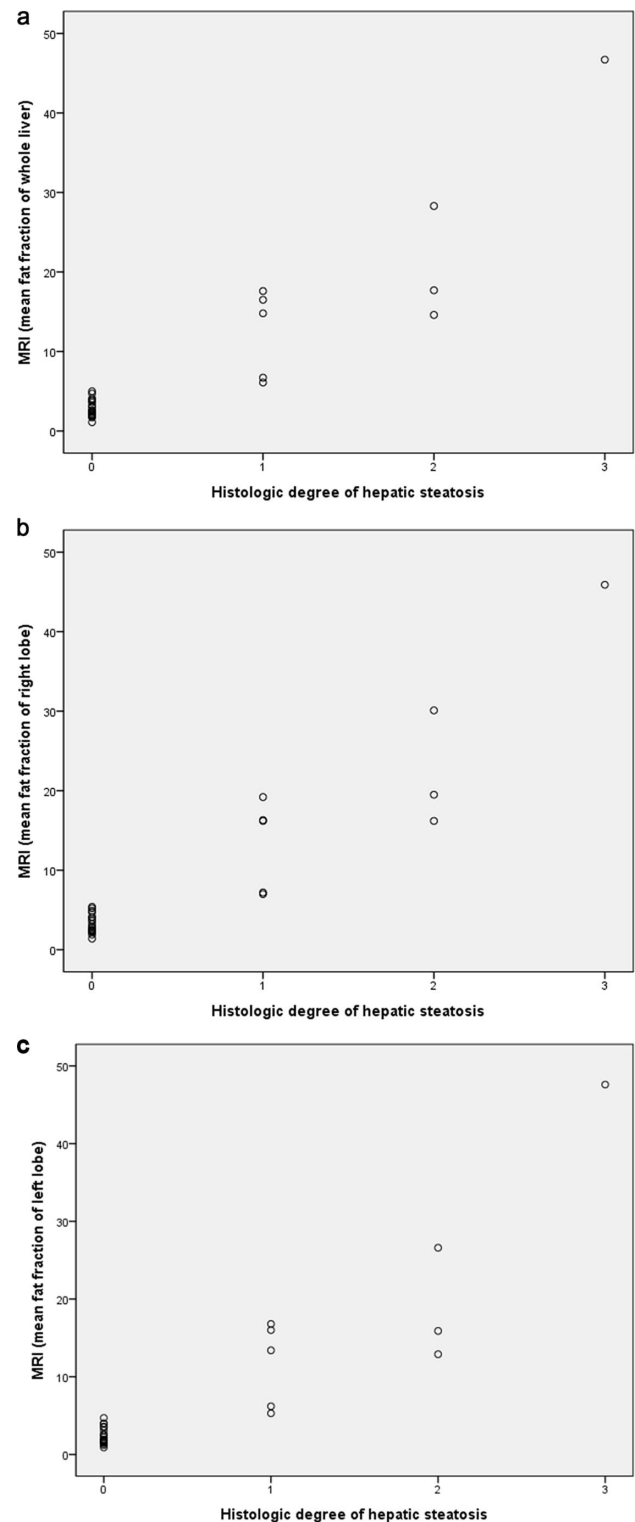


Figure 2. Linear correlation and Bland-Altman analyses of mean fat fraction measured by MRI and MRS: (a) correlation analysis and (b) Bland-Altman analysis of whole-liver PDFF and MRS; (c) correlation analysis and (d) Bland-Altman analysis of right-lobe PDFF and MRS; (e) correlation analysis and (f) Bland-Altman analysis of left-lobe PDFF and MRS; (g) correlation analysis and (h) Bland-Altman analysis of segment IV PDFF and MRS. In Bland-Altman analysis, the thick solid line represents the mean value and dashed lines represent 95% confidence intervals. PDFF, proton density fat fraction; MRS, magnetic resonance spectroscopy.

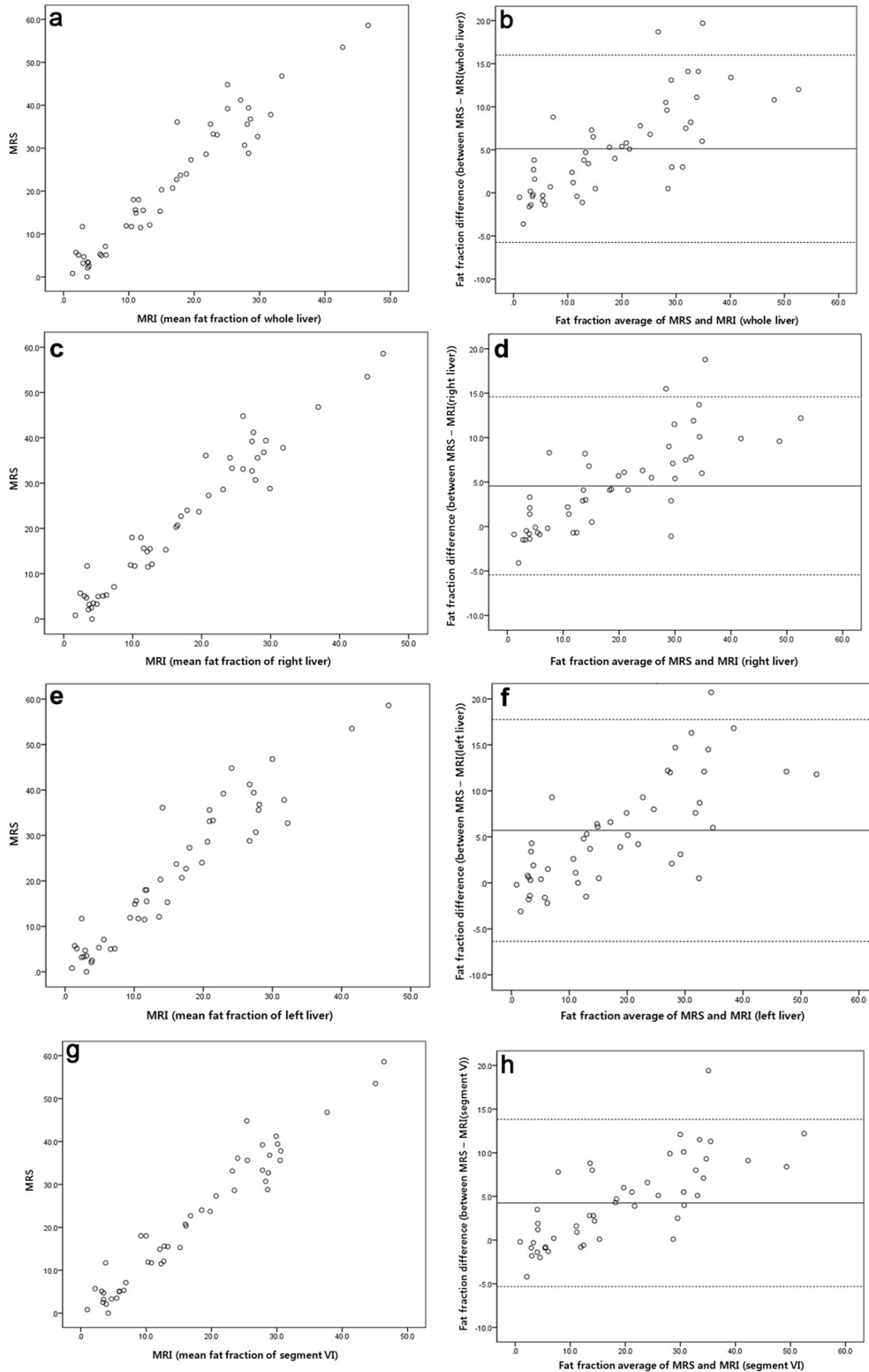


Table 3. Intrahepatic fat distribution and variability using MRI ($n = 139$ examinations)

	Fat fraction	Variability (SD)	PDFF range (Max-Min)
Whole liver	14.3 (1.1–46.7)	1.68 (0.54–6.39)	4.9 (0.8–19.5)
Lobe			
Right	14.9 (1.4–46.3)	1.15 (0.37–3.98)	2.4 (0.3–12.8)
Left	13.8 (0.7–47.6)	1.74 (0.42–8.34)	3.5 (0.3–19.5)
Segment			
I	13.8 (0.3–47)	1.14 (0.06–8.62)	2.2 (0.1–16.2)
II	13 (0.2–48.3)	1.11 (0.06–6.23)	2.1 (0.1–12)
III	13.9 (0.3–49.6)	1.19 (0.06–15.75)	2.3 (0.1–28.7)
IV	14.5 (0.2–46.9)	0.88 (0.06–4.79)	1.7 (0.1–8.8)
V	14.8 (0.3–47.5)	0.78 (0.06–5.69)	1.4 (0.1–5.9)
VI	15.1 (1–46.4)	0.66 (0–2.54)	1.3 (0–4.7)
VII	14.9 (0.9–45.7)	0.71 (0.06–2.21)	1.4 (0.1–4.3)
VIII	14.7 (0.8–45.8)	1.16 (0–15.03)	1.4 (0–3.8)

PDFF range, differences between maximum and minimum PDFF.

inflammation, fibrosis and ballooning degeneration. But its applicability is limited by its high sampling variability, poor interobserver correlations^{5,21} and its invasiveness, which includes risk of pain, bleeding and very rarely death. Additionally, histology-determined steatosis is less sensitive for detection of small changes in liver fat.¹⁵ Nouredin et al found that PDFF changes greater than 1% are correlated with changes in anthropometric and serologic markers.¹⁴ MRI-PDFF is a reliable method for detecting small differences in fat fraction and for longitudinal monitoring in clinical settings with high repeatability between examinations.^{22,23}

Our result showed PDFF variability and PDFF range increased as PDFF increased. It is thought to be an inevitable result related to non-uniform fatty deposition in the liver. Even though a heterogeneous or non-uniform distribution of steatosis is well described in the literature,²⁴ detailed descriptions of hepatic fat distribution are lacking due to the difficulty in conducting biopsy or MRS. Currently, due technical advances in MRI for hepatic fat quantification, such as MRI-PDFF, it is possible to describe intrahepatic fat distribution in high detail.

We observed significantly higher PDFF values with lower variability in the right hepatic lobe compared with the left, which is consistent with several previous studies.^{10,22,24} This may be attributed to preferential shunting of fatty mesenteric blood toward the right portal vein and shunting of splenic blood toward the left portal vein. In segmental measurement of MRI-PDFF, segment VI showed more consistent MRI-PDFF with low variability than segments close the diaphragm. We cannot exclude the possibility that motion artefacts might have influenced the measurement, despite our efforts to avoiding artefacts as much as possible when measuring ROIs. However, our results were comparable to those of Bonekamp et al, who reported spatial distribution of MRI-PDFF in 50 adults with NAFLD,⁹ and these values might be true differences. It is

speculated that the difference in oxygen gradient according to the blood supply of the liver²⁵ or a third inflow of blood other than the usual hepatic arterial and portal venous sources may affect distribution of hepatic steatosis and its variability, but further investigation is required.

Our study cohort was composed of patients with various hepatic disorders, including 40 (47.6%, 40/85) patients with NAFLD. Although our sample size was different from Bonekamp et al (50 patients with NAFLD), results were consistent between the two studies. We believe these findings raise the possibility that MRI-PDFF is a non-invasive biomarker for hepatic fat quantification in clinical settings regardless of hepatic disorder.

The most precise fat fraction measurement was achieved for the mean liver PDFF obtained by whole-liver segmentation, but this is a vexatious measurement to undertake in a clinical setting. A simple and precise monitoring method is needed. Based on our data, the right liver, especially segment VI, could be used for follow-up of liver-fat fraction because of its low fat variance, although it had a slightly higher baseline value.

Our study has several limitations. First, our study was performed on a small cohort of 85 patients; however, this cohort was relatively large compared with previous studies.^{10–12} Second, our study cohort included many hepatic disorders, which could have affected fat distribution. Although our findings are not relevant to any specific disease group, they are applicable in clinical settings that cover various hepatic disorders. Further studies are required to assess hepatic fat distribution for each disease group. Third, MRI PDFF was not compared with MRS and histology at the same location. Because MRI PDFF is often used to measure whole liver in a clinical setting, we tried to compare MRS and histology with the method actually used. MRI PDFF showed a good correlation with MRS in our study, but does not exactly

match may be due to this reason. Fourth, liver biopsies were not performed in all of our study patients, therefore colocalization of each segment could not be performed. However, liver biopsy samples are small and may lead to sampling errors.⁵ Furthermore, it would not have been ethically acceptable to perform multiple *in vivo* liver biopsies at each segment. Consideration should be made to compare biopsies and MRI PDFF in future studies using *ex vivo* tissue for whole liver fat quantification. Finally, ROI sampling methods can affect MRI-PDFF results. However, it remains unclear how to and where to measure hepatic fat fraction in a MRI-PDFF map, except that liver-fat fraction was not significantly affected by shape of ROI.¹¹

In conclusion, MRI-PDFF using the mDIXON-Quant sequence is an accurate non-invasive method of hepatic fat quantification in various hepatic disorders. Our study revealed small but significant differences in hepatic FF between lobes and segments. Segment VI had highest mean FF and lowest variability, while the left lateral segment of the liver had lower FF, higher variability, and higher PDFF range. Therefore, we conclude that it would be preferable to measure FF in the right liver, especially segment VI for precise estimates, while avoiding FF measurement in the left liver.

FUNDING

This work was supported by a research fund from the National Research Foundation of Korea 2011-0007127.

REFERENCES

1. Younossi ZM, Koenig AB, Abdelatif D, Fazel Y, Henry L, Wymer M. Global epidemiology of nonalcoholic fatty liver disease—meta-analytic assessment of prevalence, incidence, and outcomes. *Hepatology* 2016; **64**: 73–84. doi: <https://doi.org/10.1002/hep.28431>
2. Chalasani N, Younossi Z, Lavine JE, Diehl AM, Brunt EM, Cusi K, et al. The diagnosis and management of non-alcoholic fatty liver disease: practice guideline by the American Association for the Study of Liver Diseases, American College of Gastroenterology, and the American Gastroenterological Association. *Hepatology* 2012; **55**: 2005–23. doi: <https://doi.org/10.1002/hep.25762>
3. Zezos P, Renner EL. Liver transplantation and non-alcoholic fatty liver disease. *World J Gastroenterol* 2014; **20**: 15532–8. doi: <https://doi.org/10.3748/wjg.v20.i42.15532>
4. Hoppe S, von Loeffelholz C, Lock JF, Doecke S, Sinn BV, Rieger A, et al. Nonalcoholic steatohepatitis and liver steatosis modify partial hepatectomy recovery. *J Invest Surg* 2015; **28**: 24–31. doi: <https://doi.org/10.3109/08941939.2014.971206>
5. Ratziu V, Charlotte F, Heurtier A, Gombert S, Giral P, Bruckert E, et al. LIDO Study Group. Sampling variability of liver biopsy in nonalcoholic fatty liver disease. *Gastroenterology* 2005; **128**: 1898–906. doi: <https://doi.org/10.1053/j.gastro.2005.03.084>
6. Bravo AA, Sheth SG, Chopra S. Liver biopsy. *N Engl J Med* 2001; **344**: 495–500. doi: <https://doi.org/10.1056/NEJM200102153440706>
7. Reeder SB, Sirlin CB. Quantification of liver fat with magnetic resonance imaging. *Magn Reson Imaging Clin N Am* 2010; **18**: 337–357ix–357. doi: <https://doi.org/10.1016/j.mric.2010.08.013>
8. el-Hassan AY, Ibrahim EM, al-Mulhim FA, Nabhan AA, Chammas MY. Fatty infiltration of the liver: analysis of prevalence, radiological and clinical features and influence on patient management. *Br J Radiol* 1992; **65**: 774–8. doi: <https://doi.org/10.1259/0007-1285-65-777-774>
9. Décarie PO, Lepanto L, Billiard JS, Olivie D, Murphy-Lavallée J, Kauffmann C, et al. Fatty liver deposition and sparing: a pictorial review. *Insights Imaging* 2011; **2**: 533–8. doi: <https://doi.org/10.1007/s13244-011-0112-5>
10. Bonekamp S, Tang A, Mashhood A, Wolfson T, Changchien C, Middleton MS, et al. Spatial distribution of MRI-Determined hepatic proton density fat fraction in adults with nonalcoholic fatty liver disease. *J Magn Reson Imaging* 2014; **39**: 1525–32. doi: <https://doi.org/10.1002/jmri.24321>
11. Vu KN, Gilbert G, Chalut M, Chagnon M, Chartrand G, Tang A. MRI-determined liver proton density fat fraction, with MRS validation: comparison of regions of interest sampling methods in patients with type 2 diabetes. *J Magn Reson Imaging* 2016; **43**: 1090–9. doi: <https://doi.org/10.1002/jmri.25083>
12. Tang A, Tan J, Sun M, Hamilton G, Bydder M, Wolfson T, et al. Nonalcoholic fatty liver disease: MR imaging of liver proton density fat fraction to assess hepatic steatosis. *Radiology* 2013; **267**: 422–31. doi: <https://doi.org/10.1148/radiol.12120896>
13. Kang BK, Yu ES, Lee SS, Lee Y, Kim N, Sirlin CB, et al. Hepatic fat quantification: a prospective comparison of magnetic resonance spectroscopy and analysis methods for chemical-shift gradient echo magnetic resonance imaging with histologic assessment as the reference standard. *Invest Radiol* 2012; **47**: 368–75. doi: <https://doi.org/10.1097/RLI.0b013e31824baff3>
14. Yokoo T, Shiehmorteza M, Hamilton G, Wolfson T, Schroeder ME, Middleton MS, et al. Estimation of hepatic proton-density fat fraction by using MR imaging at 3.0 T. *Radiology* 2011; **258**: 749–59. doi: <https://doi.org/10.1148/radiol.10100659>
15. Noureddin M, Lam J, Peterson MR, Middleton M, Hamilton G, Le TA, et al. Utility of magnetic resonance imaging versus histology for quantifying changes in liver fat in nonalcoholic fatty liver disease trials. *Hepatology* 2013; **58**: 1930–40. doi: <https://doi.org/10.1002/hep.26455>
16. Kukuk GM, Hittatiya K, Sprinkart AM, Eggers H, Gieseke J, Block W, et al. Comparison between modified Dixon MRI techniques, MR spectroscopic relaxometry, and different histologic quantification methods in the assessment of hepatic steatosis. *Eur Radiol* 2015; **25**: 2869–79. doi: <https://doi.org/10.1007/s00330-015-3703-6>
17. Di Martino M, Pacifico L, Bezzi M, Di Miscio R, Sacconi B, Chiesa C, et al. Comparison of magnetic resonance spectroscopy, proton density fat fraction and histological analysis in the quantification of liver steatosis in children and adolescents. *World J Gastroenterol* 2016; **22**: 8812–9. doi: <https://doi.org/10.3748/wjg.v22.i39.8812>
18. Permutt Z, Le TA, Peterson MR, Seki E, Brenner DA, Sirlin C, et al. Correlation between liver histology and novel magnetic resonance imaging in adult patients with non-alcoholic fatty liver disease - MRI accurately quantifies hepatic steatosis in NAFLD. *Aliment Pharmacol Ther* 2012; **36**:

- 22–9. doi: <https://doi.org/10.1111/j.1365-2036.2012.05121.x>
19. Idilman IS, Keskin O, Celik A, Savas B, Halil Elhan A, Idilman R, et al. A comparison of liver fat content as determined by magnetic resonance imaging-proton density fat fraction and MRS versus liver histology in non-alcoholic fatty liver disease. *Acta Radiol* 2016; **57**: 271–8. doi: <https://doi.org/10.1177/0284185115580488>
20. Kramer H, Pickhardt PJ, Kliewer MA, Hernando D, Chen GH, Zagzebski JA, et al. Accuracy of Liver Fat Quantification With Advanced CT, MRI, and Ultrasound Techniques: Prospective Comparison With MR Spectroscopy. *AJR Am J Roentgenol* 2017; **208**: 92–100. doi: <https://doi.org/10.2214/AJR.16.16565>
21. Juluri R, Vuppalanchi R, Olson J, Unalp A, Van Natta ML, Cummings OW, et al. Generalizability of the nonalcoholic steatohepatitis clinical research network histologic scoring system for nonalcoholic fatty liver disease. *J Clin Gastroenterol* 2011; **45**: 55–8. doi: <https://doi.org/10.1097/MCG.0b013e3181dd1348>
22. Sofue K, Mileto A, Dale BM, Zhong X, Bashir MR. Interexamination repeatability and spatial heterogeneity of liver iron and fat quantification using MRI-based multistep adaptive fitting algorithm. *J Magn Reson Imaging* 2015; **42**: 1281–90. doi: <https://doi.org/10.1002/jmri.24922>
23. Hernando D, Sharma SD, Aliyari Ghasabeh M, Alvis BD, Arora SS, Hamilton G, et al. Multisite, multivendor validation of the accuracy and reproducibility of proton-density fat-fraction quantification at 1.5T and 3T using a fat-water phantom. *Magn Reson Med* 2017; **77**: 1516–24. doi: <https://doi.org/10.1002/mrm.26228>
24. Bannas P, Kramer H, Hernando D, Agni R, Cunningham AM, Mandal R, et al. Quantitative magnetic resonance imaging of hepatic steatosis: validation in ex vivo human livers. *Hepatology* 2015; **62**: 1444–55. doi: <https://doi.org/10.1002/hep.28012>
25. Anavi S, Madar Z, Tirosh O. Non-alcoholic fatty liver disease, to struggle with the strangle: Oxygen availability in fatty livers. *Redox Biol* 2017; **13**: 386–92. doi: <https://doi.org/10.1016/j.redox.2017.06.008>